

Photoluminescence line shape of excitons in alloy semiconductors

E. F. Schubert* and W. T. Tsang
AT&T Bell Laboratories, Holmdel, New Jersey 07733
 (Received 9 April 1986)

The study of low-temperature photoluminescence spectra of $\text{Ga}_{47}\text{In}_{53}\text{As}$ as a function of excitation intensity reveals three distinct features: With decreasing excitation intensity the excitonic line (i) narrows, (ii) shifts to lower energies, and (iii) gets increasingly asymmetric. This behavior is more pronounced in samples with a broad excitonic linewidth. At low excitation intensities linewidths of 1.2 meV for $\text{Ga}_{47}\text{In}_{53}\text{As}$ grown by chemical-beam epitaxy are found. The experimental observations are described in terms of a quantitative, semiclassical model which is based on the migration of carriers to low-energy sites of the zinc blende alloy. An expression for the photoluminescence line shape of excitons in alloy semiconductors is given for the first time. The experimental results are well described by this theoretical model.

Ternary and quaternary III-V alloy semiconductors are one example of materials with a perturbed crystal potential. The perturbation results from microscopic, statistical variations of the alloy composition.¹⁻³ Other examples of statistically disordered semiconductors are (i) highly doped semiconductors, (ii) quantum wells with a fluctuating well width, and (iii) the amorphous state of semiconductors. This microscopic variation of the alloy composition strongly affects the linewidth of excitons in low-temperature photoluminescence spectra. The linewidth of bound excitons is less than 0.1 meV in binary III-V semiconductors,⁴ while it is several meV in the alloy-broadened spectra of ternaries and quaternaries.⁵⁻⁷ The line shape of bound excitons in a binary semiconductor is given by the Lorentzian function. In the $\text{Al}_x\text{Ga}_{1-x}\text{As}$ alloy the line shape was shown to be Gaussian at a sufficiently high excitation intensity.¹ Currently, high-quality alloy materials grown by chemical-beam epitaxy are a useful tool to study the optical properties of excitons in pseudobinary cation alloys.⁸

In this Rapid Communication we report the first experimental and theoretical investigation of the line shape of excitons in the alloy $\text{Ga}_{47}\text{In}_{53}\text{As}$ grown by chemical-beam epitaxy (CBE).⁸ The good quality of CBE-grown $\text{Ga}_{47}\text{In}_{53}\text{As}$ allows us to investigate the dependence of the excitonic linewidth, peak energy, and line shape on the excitation density. The experimental findings are analyzed using a semiclassical quantitative model taking into account the migration of excitons to low-energy sites of the crystal. A mathematical expression for the line shape of excitons in alloy semiconductors is derived.

High-quality ternary alloy $\text{Ga}_{47}\text{In}_{53}\text{As}$ lattice-matched to the InP substrate by CBE (Ref. 8) is used in this study. The growth velocity of the epitaxial layers is typically 3.3–3.6 $\mu\text{m}/\text{h}$. Their thicknesses are several micrometers. A systematic variation of crystal growth parameter, such as the substrate temperature of the III-V element flux ratio, is not performed in this study. Photoluminescence measurements are performed with the samples immersed into liquid He pumped to a temperature of 2 K. The 647.1-nm line of a Kr^+ laser is used for optical excitation. The laser-light spot on the sample has a diameter of 50 μm . The spontaneous luminescence light is analyzed with

a cooled Ge detector attached to a 1-m single-pass monochromator.

Experimental results of a homogeneous $\text{Ga}_{47}\text{In}_{53}\text{As}$ sample are shown in Fig. 1(a) for an excitation intensity of 10 μW . The low-temperature photoluminescence spectrum consists mainly of an excitonic line. The weak impurity-related optical transitions at an excitation power of 10 μW indicates the high purity of the CBE-grown $\text{Ga}_{47}\text{In}_{53}\text{As}$. At an excitation power of 100 nW (i.e., 5 mW/cm^2), as shown in Fig. 1(b), an impurity-assisted transition occurs at 15.8 meV below the exciton. This transition is usually referred to a donor-to-acceptor transition.^{9,10} Reduction of the exciting power from 10 μW in Fig. 1(a) to 100 nW in Fig. 1(b) shows a shift of the bound-exciton peak energy to a lower energy. In addition the linewidth of the bound exciton reduces from 2.6 to 1.9 meV. The change of the excitonic line shapes with excitation intensity is shown in detail in the inset of Fig. 1(b). The line shape changes predominantly on the high-energy side, while the low-energy side remains unchanged. The

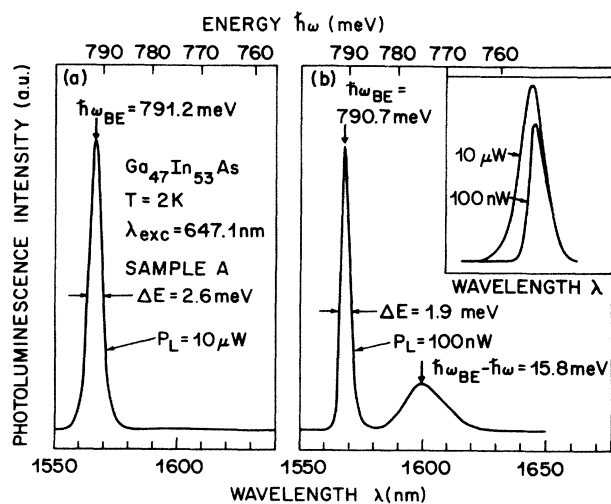


FIG. 1. Low-temperature photoluminescence spectra of undoped $\text{Ga}_{47}\text{In}_{53}\text{As}$. The excitation intensities are (a) 10 μW (510 mW/cm^2) and (b) 100 nW (5.1 mW/cm^2). The inset shows the bound-exciton transitions for both excitation intensities and a magnified abscissa scale.

changes of the linewidths and of the peak energies as a function of excitation density is shown in Fig. 2 for three samples. For sample *A*, which has a narrow excitonic linewidth, the shift of the peak energy is approximately 0.27 meV per decade excitation intensity. For sample *B*, which has a broader linewidth ($\Delta E_{\text{exc}} \approx 6$ meV), the shift of the peak energy amounts to 0.5 meV per decade excitation intensity. Sample *C* has an extremely narrow linewidth of 1.2 meV (at 100-nW excitation power) and a shift of the peak energy of 0.05 meV per decade excitation intensity. Consequently, the line-narrowing and the peak-energy shift in the three samples are proportional to the linewidths.

The narrow photoluminescence spectra of a $\text{Ga}_{47}\text{In}_{53}\text{As}$ (sample *C*) layer is shown in Fig. 3. At an excitation intensity of 5 mW/cm^2 , the linewidth (full width at half maximum), is 1.2 meV. It is noteworthy that this linewidth is the narrowest reported so far for $\text{Ga}_{47}\text{In}_{53}\text{As}$. The $\text{Ga}_{47}\text{In}_{53}\text{As}$ layer thickness of sample *C* is $0.2 \mu\text{m}$ and the ternary layer is clad by InP. We attribute the narrow linewidth of sample *C* partly to the thin $\text{Ga}_{47}\text{In}_{53}\text{As}$ layer which makes composition fluctuations along the growth axis less effective. Band-filling effects of the Burstein shift are excluded as origin of the energy shift of the excitonic line, because all measurements are performed at low-excitation intensities. Hot carrier luminescence is excluded as well at the power densities used in this study. Next we will outline a quantitative semiclassical model that explains the observed properties of excitons in alloy semiconductors.

The linewidth of an exciton in a random alloy semiconductor was calculated by assuming statistical distribution of cations in the zinc blende lattice. The alloy-broadened

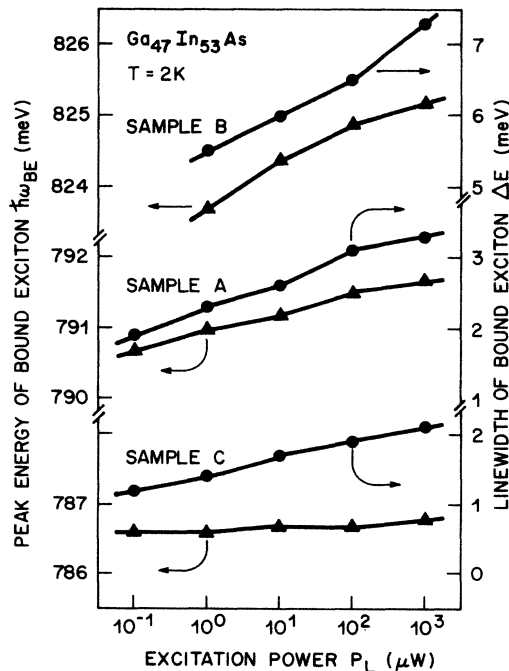


FIG. 2. Dependence of peak energy and linewidth of the bound-exciton transition in $\text{Ga}_{47}\text{In}_{53}\text{As}$ on the excitation intensity for the three samples. The narrowest bound-exciton linewidth obtained is 1.2 meV.

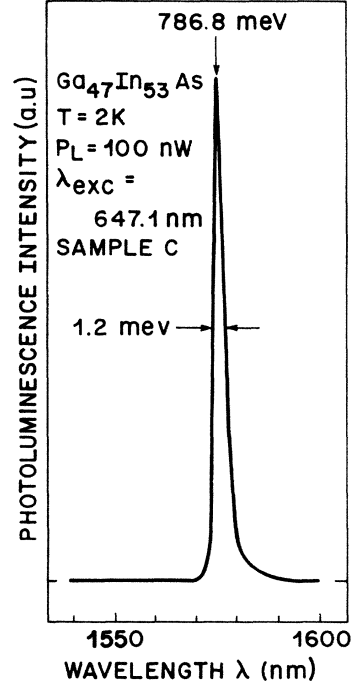


FIG. 3. Low-temperature photoluminescence spectrum of an undoped $0.2\text{-}\mu\text{m}$ -thick $\text{Ga}_{47}\text{In}_{53}\text{As}$ layer clad by InP barriers.

linewidth of excitons reflects the compositional variation of the band-gap energy in real space. The varying energy gap is shown schematically in Fig. 4(a). Assuming that all charge carriers are *distributed homogeneously* in the semiconductor, i.e., carriers do not *preferentially* occupy low-energy states in the crystal, the excitonic linewidth is given by¹

$$\Delta E_{\text{exc}} = 2.36\sigma_E = 2.36 \frac{dE_g}{dx} \left(\frac{x(1-x)}{4a_0^{-3} \left(\frac{4}{3}\right)\pi a_{\text{exc}}^3} \right)^{1/2}, \quad (1)$$

where dE_g/dx is the change of the energy gap with the alloy composition x , a_0 is the lattice constant, and a_{exc} is the excitonic radius. Using the hydrogen model for determination of the excitonic radius the photoluminescence linewidth of an exciton in $\text{Ga}_{47}\text{In}_{53}\text{As}$ is $\Delta E_{\text{exc}} = 1.6$ meV. In $\text{Ga}_{47}\text{In}_{53}\text{As}$ there might be additional variations of the alloy compositions not explainable by statistics, as pointed out by Penna *et al.*¹¹ Therefore, the standard energy deviation σ_E for $\text{Ga}_{47}\text{In}_{53}\text{As}$ might be larger¹¹ than expected from Eq. (1). Homogeneous carrier distribution within the random alloy potential yields an exciton line shape of Gaussian form,

$$f(E) = 1/(\sigma_E\sqrt{2\pi}) \exp \left[-\frac{1}{2} \left(\frac{E - E_{\text{exc}}}{\sigma_E} \right)^2 \right], \quad (2)$$

with σ_E given by Eq. (1). Equation (2) is reminiscent of Urbach's law,¹² which points out that there is an exponentially decreasing density of states close to the fundamental gap of a semiconductor. Furthermore, Eq. (2) does not comply with Nordheim's rule,¹³ which states that an effect due to alloy disorder should be symmetric with x . If there is a considerable bowing of the energy gap with x , Nordheim's rule does not apply. The experimental results

described above do not suggest anymore of a homogeneous carrier distribution in the crystal. Instead, a preferential recombination from low-energy sites of the crystal is expected at low-excitation intensities.

Next, we will take into account the migration of electron-hole pairs into the low-energy valleys of the crystal as schematically shown in Fig. 4(a). When electron-hole pairs are excited high into the conduction and valence band, energy relaxation occurs rapidly due to optical-phonon scattering within times on the order of 0.1 ps. After relaxation the carriers are consequently distributed homogeneously in real space. At high-excitation intensity the van Roosbroeck-Shockley recombination lifetime is short, and no preferential recombination from a low-energy site occurs. The photoluminescence spectrum then represents the distribution of the energy gap in space. In this case, the peak energy of excitonic luminescence and absorption spectra nearly coincide¹⁴ as long as no impurity-related transitions and no Burstein shift occur.

$$I(E) = \exp\left[-\frac{1}{2}\left(\frac{E - E_{exc}}{\sigma_E}\right)^2\right] \exp\left\{-\frac{\tau_r}{\tau_c}\left[\frac{1}{\sigma_E\sqrt{2\pi}}\int_{-\infty}^E \exp\left[-\frac{1}{2}\left(\frac{E^* - E_{exc}}{\sigma_E}\right)^2\right] dE^*\right]\right\}. \quad (4)$$

Since the recombination time τ_r in turn depends on the excitation intensity, the ratio τ_r/τ_c can be tuned by changing the excitation intensity. Figure 4(b) shows some luminescence line shapes for the exciton according to Eq. (4) with

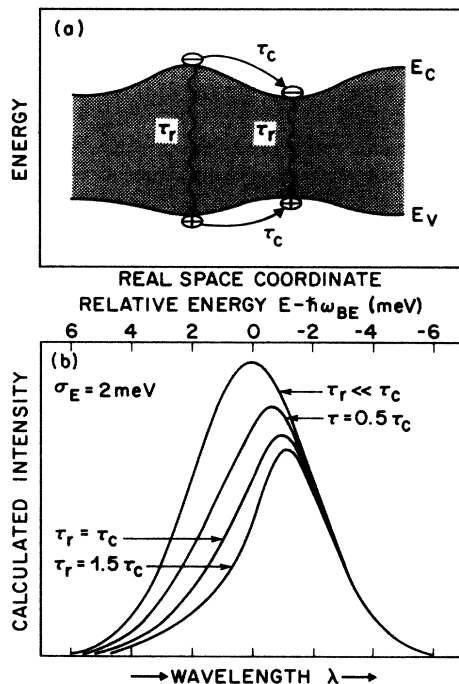


FIG. 4. (a) Schematic sketch of varying conduction and valence-band edges due to statistical fluctuations of the alloy composition. The carriers migrate to low-energy sites of the crystal within a time τ_c , which is assumed to be equal for electrons and holes. The time τ_r denotes the radiative recombination lifetime. (b) Theoretical line shape of excitons in alloy semiconductors according to Eq. (4) for various ratios τ_r/τ_c . For $\tau_r \ll \tau_c$ the excitonic band is of Gaussian shape.

At low-excitation intensities, the lifetime of carriers is, however, long, and energy relaxation within the distorted crystal takes place. The characteristic time constant for carriers to migrate into valleys is taken to be τ_c . The change of a given carrier concentration (or exciton concentration) at a given energy E and time t , $[dn(E,t)]/dt$, can be expressed by a nonlinear first-order partial differential rate equation,

$$\frac{dn(E,t)}{dt} = [-F(E)] \frac{1}{\tau_c} n(E,t), \quad (3)$$

where $F(E)$ is the distribution function

$$F(E) = \int_{-\infty}^E f(E) dE,$$

and $F(E)$ represents the availability of states lower than E .

Solving Eq. (3) with the boundary condition $n(E,0) = n_0 f(E)$ yields the spectral shape of excitonic recombination in alloy semiconductors, i.e., at $t = \tau_r$:

various ratios τ_r/τ_c . For long recombination lifetimes ($\tau_r > \tau_c$, i.e., low-intensity excitation) the radiative transitions occur predominantly from low-energy sites of the crystal. Qualitatively, the calculated photoluminescence spectrum of Fig. 4(b) coincides with the measured excitonic photoluminescence spectrum, as shown in the inset of

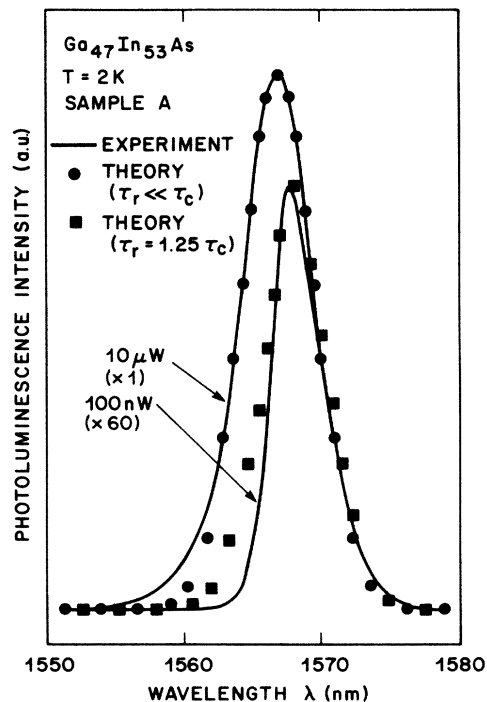


FIG. 5. Comparison of experimental low-temperature photoluminescence spectra (solid lines) of $\text{Ga}_{47}\text{In}_{53}\text{As}$ at the excitation intensities $10 \mu\text{W}$ (510 mW/cm^2) and 100 nW (5.1 mW/cm^2) with their theoretical fit (filled circles and squares) according to Eq. (4) with $\sigma_E = 1.1 \text{ meV}$.

Fig. 1(b), in terms of (i) line narrowing, (ii) shift of peak energy, and (iii) change of the emission band at the high-energy side of the spectrum. The theoretical result of Eq. (4) is fitted to experimental results by adjusting the time ratio τ_r/τ_c . Experimental measurements (10 μ W and 100 nW, solid line) are shown together with their theoretical fit (filled circles and squares) in Fig. 5. The agreement includes the (i) line narrowing, (ii) peak-energy shift, and (iii) the change of the exciton band predominantly on its high-energy side, i.e., the asymmetric change of the exciton band. Minor discrepancies on the high-energy side of the low-intensity spectrum are probably due to reabsorption of photons in the epitaxial layer. The spectrum obtained at an excitation power of 1 μ W (not shown in Fig. 5) yields a good agreement with the theoretical fit as well.

The time of exciton formation is not critical in the above model, since both excitons and free carriers tend to occupy preferentially the low-energy sites of the alloy. In impurity bound excitons the binding of the exciton to the impurity is strongly reduced in the alloy due to electric fields via the Poole-Frenkel effect.¹ Therefore, also impurity-bound excitons could diffuse to the energy valleys. The

phenomenological, semiclassical model described here explains all observed experimental results.

In conclusion, the study of low-temperature photoluminescence spectra of excitons in Ga₄₇In₅₃As reveals a (i) line narrowing, (ii) shift of the peak energy, and (iii) an asymmetric change of the line shape by lowering the excitation intensity. Both the amount of line narrowing and peak-energy shift are proportional to the linewidth itself. The narrow excitonic linewidths of $\Delta E = 1.2$ meV reveal the superior quality of Ga₄₇In₅₃As grown by chemical-beam epitaxy. The experimental results are analyzed in terms of a quantitative semiclassical model that takes into account the migration of carriers into the low-energy sites of the crystal. The line shape of exciton recombination in alloy semiconductors is determined by a partial differential rate equation and is given in analytic form for the first time. The theoretical model coincides with all experimental findings.

The authors would like to thank J. Shah for excellent cooperation and A. DiGiovanni for helpful technical assistance.

*On leave from Max-Planck-Institut für Festkörperforschung, Stuttgart, Federal Republic of Germany.

¹E. F. Schubert, E. O. Goebel, Y. Horikoshi, K. Ploog, and H. J. Queisser, *Phys. Rev. B* **30**, 813 (1984); E. F. Schubert and K. Ploog, *J. Phys. C* **18**, 4549 (1985).

²M. Teicher, R. Besermann, M. V. Klein, and H. Morkoc, *Phys. Rev. B* **29**, 4652 (1984).

³Y. Kashihara, N. Kashiwagura, M. Sakata, J. Harada, and T. Arii, *Jpn. J. Appl. Phys.* **23**, L901 (1984).

⁴See, e.g., M. D. Sturge, in *Excitons*, edited by E. I. Rashba and M. D. Sturge (North-Holland, Amsterdam, 1982), p. 3; H. B. Bebb and E. W. Williams, in *Semiconductors and Semimetals*, edited by R. K. Willardson and A. C. Beer (Academic, New York, 1972), p. 321.

⁵R. J. Nelson, in *Excitons*, edited by E. I. Rashba and M. D. Sturge (North-Holland, Amsterdam, 1982), p. 319.

⁶R. C. Miller and W. T. Tsang, *Appl. Phys. Lett.* **39**, 334 (1981).

⁷E. O. Goebel, in *GaInAsP Alloy Semiconductors*, edited by

T. P. Pearsall (Wiley, New York, 1982), p. 313.

⁸W. T. Tsang, *Appl. Phys. Lett.* **45**, 1236 (1984).

⁹V. Swaminathan, R. A. Stall, A. T. Macrander, and R. J. Wunder, *J. Vac. Sci. Technol. B* **3**, 1631 (1985).

¹⁰A. F. S. Penna, J. Shah, A. E. DiGiovanni, A. G. Dentai, *Solid State Commun.* **51**, 217 (1984).

¹¹A. F. S. Penna, J. Shah, T. Y. Chang, and M. S. Burroughs, R. E. Nahory, M. Tamargo, and H. M. Cox, *Solid State Commun.* **51**, 425 (1984).

¹²In 1953, Urbach established empirically the exponential dependence of the absorption coefficient on the photon energy near the long-wave fundamental absorption edge of alkali-halide crystals. It has been found that this behavior of the absorption is not specific to alkali halides but is observed also in semiconductors. See, F. Urbach, *Phys. Rev.* **92**, 1324 (1953).

¹³A. A. Mbaye, F. Raymond, and C. Verie, *Solid State Commun.* **50**, 459 (1984).

¹⁴J. Shah (private communication).

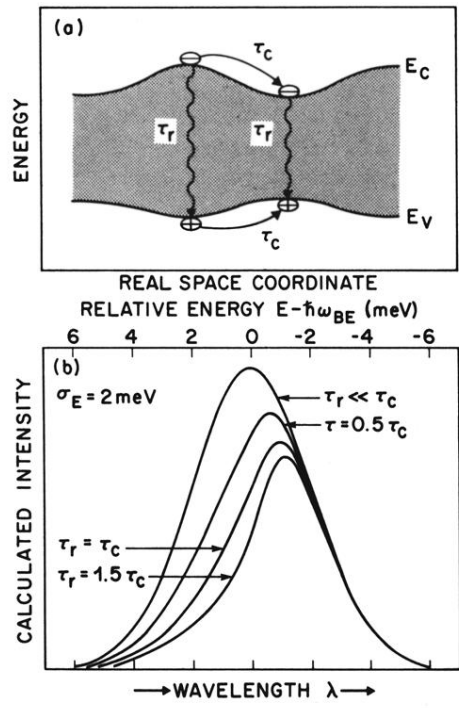


FIG. 4. (a) Schematic sketch of varying conduction and valence-band edges due to statistical fluctuations of the alloy composition. The carriers migrate to low-energy sites of the crystal within a time τ_c , which is assumed to be equal for electrons and holes. The time τ_r denotes the radiative recombination lifetime. (b) Theoretical line shape of excitons in alloy semiconductors according to Eq. (4) for various ratios τ_r/τ_c . For $\tau_r \ll \tau_c$ the excitonic band is of Gaussian shape.